SHAFT VIBRATIONS IN TURBOMACHINERY EXCITED BY CRACKS

Burkhard Grabowski
Institut für Mechanik
Universität Hannover
Hannover, Federal Republic of Germany

SUMMARY

During the past years the dynamic behavior of rotors with cracks has been investigated mainly theoretically. This paper deals with the comparison of analytical and experimental results of the dynamics of a rotor with an artificial crack. The experimental results verify the crack model used in the analysis. They show the general possibility to determine a crack by extended vibration control.

INTRODUCTION

Frequently cracks in turbine rotors have been found. Nevertheless, until now it is not really known, how cracks can be recognized early enough so that large ensuing damage can be prevented.

The latest greater damage in Germany occured in the nuclear power plant in Würgassen (ref. 1). For one year the plant had to be put out of operation because two new rotors had to be produced. Both of the LP-rotors had a crack in about the middle of the shaft. A higher level of vibration amplitudes at running speed was noticed and during rundown the resonance amplitudes were very large, but these vibrations were not assumed to be caused by a crack. The crack has been discovered accidentally. This demonstrates the unawareness of the influence of a crack on the vibrational behavior of a shaft. Certainly there is to take into account that cracks in practice are comparatively rare. On the other hand Stodola (ref. 2) in 1922 has already shown on principle the effect of a crack and these investigations were continued by other authors (refs. 3, 4, 5).

As far as known the first measurement results of a rotating shaft with a crack were published by Mayes and Davies (ref. 6) in September 1980 and at last by Inagaki et.al. in September, 1981 (ref. 7). Like in Würgassen an abnormal increase in shaft vibration was noticed in many other cracked rotors. But in some cases the warning signs were too small and some rotors were broken. Some turbine plants even virtually exploded and fragments of the shafts flew away upto a few hundred meters. Henry and Okah-Avae (ref. 8) also present cases in which deep cracks have been found without any influence on vibration amplitudes.

The cause for shaft vibrations due to a crack is the asymmetric cross section at the crack position in connexion with the self-weight of the shaft. Depending on the depth of the crack, on its position and on the damping of the system, the crack can excite small or large vibration amplitudes or the system can even become unstable.

CRACK MODEL

For a location above the horizontal diameter, the crack is subjected to only compression and the entire cross-section is supporting. When further rotated, a part of the crack area opens. A model according to figure 1 was selected to present this gradual change. At the angle of $\varphi = 90^{o}$ the complete opening of the crack is assumed. Thus in the range between $\varphi = 90^{o}$ and $\varphi = 270^{o}$ the simple model for the complete gaping crack is taken for valid. Due to the opening and closing of the crack area we call it a breathing crack in opposite to an always gaping crack, e.g. a cut.

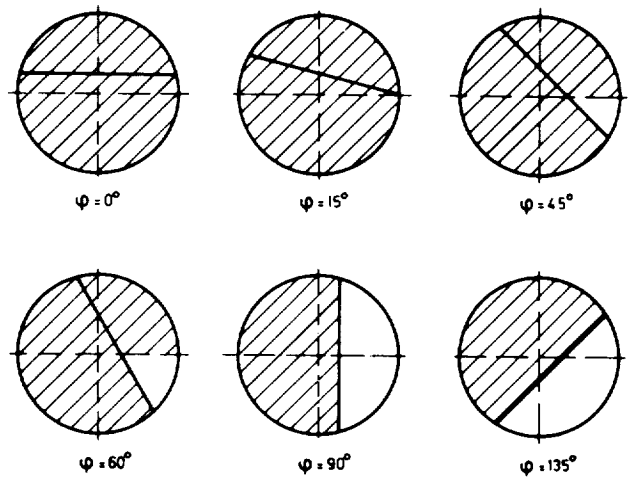

Figure 1. - Crack model cross-sections showing rotation-angle-dependent stressed regions (shaded areas).

The main axes of the second moments of area at the crack position are not fixed to the body anymore. However, this fact will have no influence on the numerical calculation, since space-fixed coordinates will be used anyway because of the non-conservative sleeve bearings. The second moments of area along the vertical and horizontal axes and the deviation moment are needed.

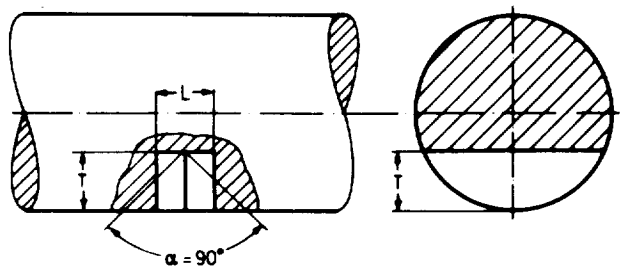

Figure 2. - Simulation of decreased cross-section open crack location.

When the crack opens the change in stiffness along the axis of the rotor does not jump, but the change is continuous in the neighbouring range. Buerhop (ref. 9) examined the effects of such cross-sections in more detail and has come to the conclusion that the 45° approximation (wedge angle $\alpha = 90^{o}$) which has been applied up to now, is sufficient. In order to simplify the mathematical model, the wedge-shaped cut-out in figure 2 is approximately replaced by a square cut with $L = T$.

A clear picture of the stiffness depending on the angle of rotation can be attained when observing the static deflection of the cracked shaft due to its self-weight during one revolution.

Where a constant gaping crack is concerned, the shaft would move on a circular orbit twice per revolution. Where a breathing crack is concerned, the shaft moves only once on an onion-shaped orbit. The calculated curves of deflection in figure 3 are in good agreement with measured results of Ziebarth et. al. (ref. 10). In order to compare the shapes of the two curves the level of the measured and the calculated amplitudes have been equalized.

In addition to the development of the theoretical crack model the stiffness of a cracked shaft has been investigated. In a shaft of 46 mm diameter and 300 mm length (fig. 4) the crack was simulated by a thin milled transverse cut of 0,5 mm width. This shaft was loaded in such a way that near the crack a constant bending moment existed.

Parallel to these measurements the stiffness of the shaft with a gaping crack has been calculated. At the crack position a square cut with L = T was assumed, but only for crack depths up to 50 percent. For deeper cracks L has to be reduced analogically.

In figure 5 the results of measurement and calculation are compared. The total compliance of the shaft depending on the crack depth is plotted. The difference between measurement and calculation amounts to less than 10 percent, except for crack depths of 20 and 70 percent. In consideration of the simple crack model even with these differences the agreement is remarkably good.

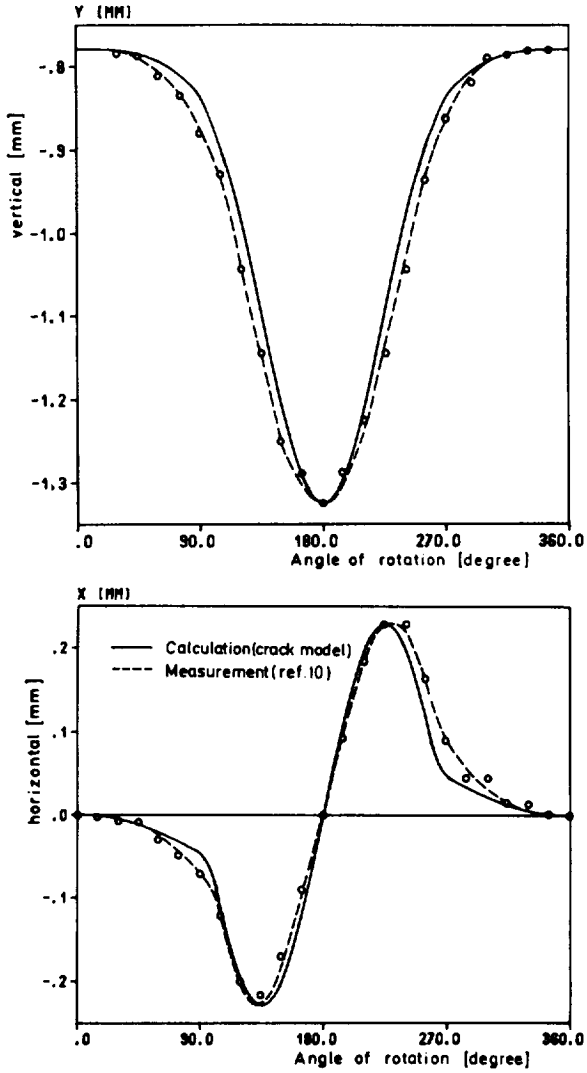

Figure 3. - Example for self-weight deflection for a breathing crack of 50 percent depth.

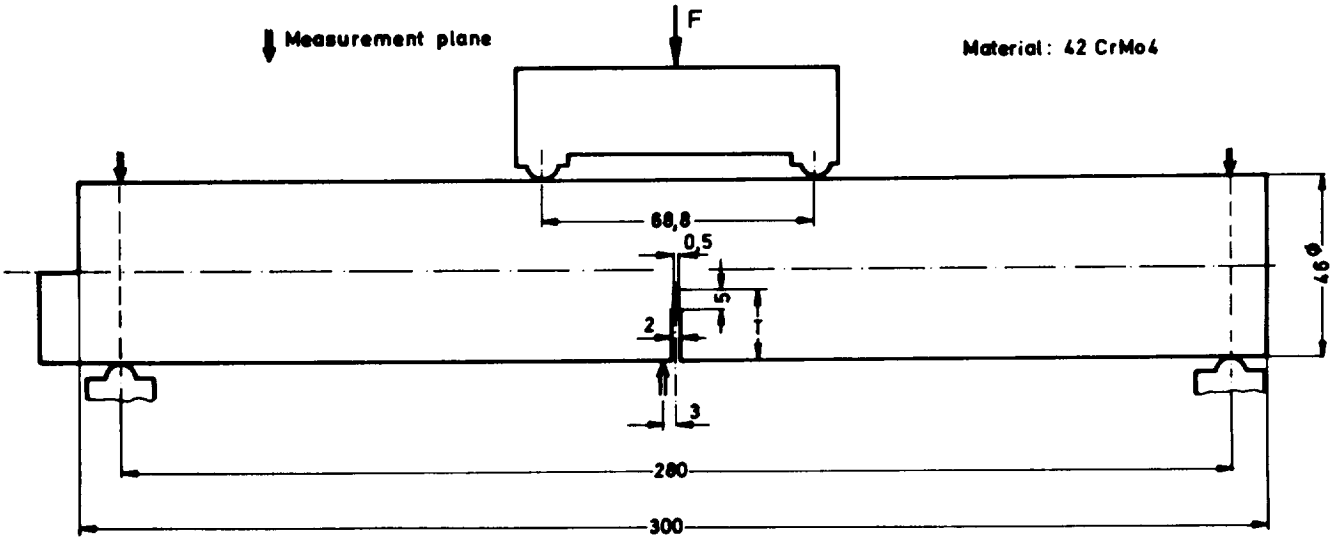

Figure 4. - Shaft with milled cut.

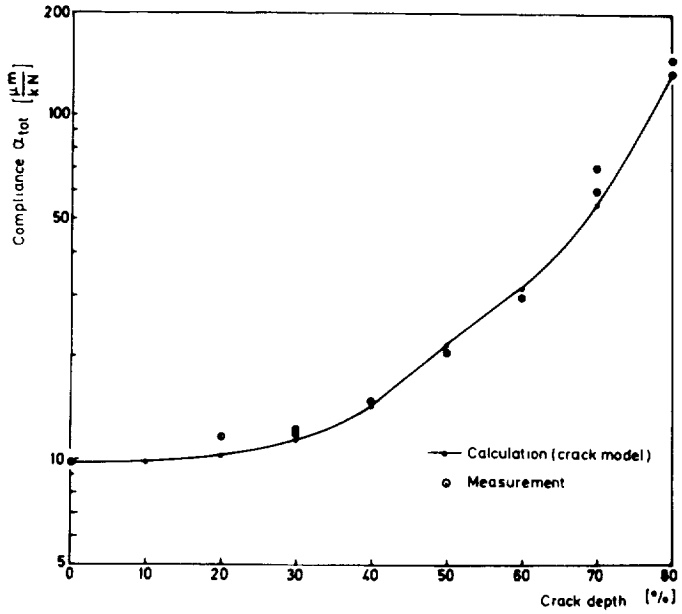

Figure 5. - Compliance α_{tot} of shaft depending on crack depth.

ANALYSIS

The mathematical model for a real rotor with cracked cross-section is a system of differential equations with time dependent coefficients. An exact solution is not possible. The vibrational behavior can, however, be calculated by means of numerical integration. For a large system, this kind of procedure with digital calculation takes a lot of time. Therefore, the behavior of the rotor can be described by its first few eigenfunctions, where the eigenfunctions $Y_o(x)$ and $Z_o(x)$ of the uncoupled conservative system for the vertical and the horizontal planes are a good approximation.

The range of the local change of stiffness due to a crack covers the length L. A mean stiffness between open and closed crack will be taken approximately for the calculation of the eigenfunctions in this region. This is necessary for the consideration of the major curvature at the crack position, compared with the uncracked shaft.

The deflections in the vertical direction $y(x,t)$ and in the horizontal direction $z(x,t)$ will be composed by the first few eigenfunctions weighted with the generalized time dependent coordinates $q(t)$, as follows

$$y(x,t) = \sum_{k=1}^{K} Y_{ok}(x)\, q_{yk}(t) \tag{1}$$

$$z(x,t) = \sum_{\ell=1}^{L} Z_{o\ell}(x)\, q_{z\ell}(t) \tag{2}$$

The transformation, which includes the complete bearing stiffness and damping coefficients, yields a system of $K + L$ coupled equations of motion for the generalized coordinates $q(t)$ which is

$$M\ddot{q} + C\dot{q} + K(t)q = F(t) + g \quad . \tag{3}$$

M, C and K can be considered as mass matrix, damping matrix and stiffness matrix. On the right-hand side the function F(t) includes the out-of-balance distribution, while g contains the self-weight load.

The time dependent elements in the stiffness matrix K(t) can be separated and we obtain

$$M\ddot{q} + C\dot{p} + [K_m + \Delta K(t)]q = F(t) + g \quad . \tag{4}$$

A Runge-Kutta-Fehlberg procedure of 5th order with constant step-size (ref. 11) which proved to be very exact for the necessary computing time, will be used by the numerical integration for the calculation of the instationary vibrational behavior. The necessary initial values will be taken from the stationary solution of equation (4) without the term $\Delta K(t)$. The time variable system has a stationary periodic solution.

After the retransformation according to equations (1) and (2) the deflection of the entire rotor which depends on the angle of rotation is obtained. The first few harmonics for certain positions on the rotor can be determined by means of Fourier analysis.

A detailed presentation of the mathematical method is given in references 11 and 13. Additional theoretical results are in references 13 and 14.

EXPERIMENTAL AND THEORETICAL INVESTIGATIONS

Experimental Rotor and Crack Propagation

To confirm the theoretical results of the vibrational behavior of cracked shafts experimental investigations were carried out. Figure 6 shows the experimental rotor, which is supported by journal bearings in an experimental Helium-compressor housing. At first it was intended to produce the crack by an oscillating load. However, other experiments with this kind of load have shown, that a crack surface due to such a treatment is different from a crack surface which is produced by an alternating load. Therefore, we decided to produce the crack during the rotation of the shaft in the rig itself by application by an external force.

Due to the high bearing load as a result of the external force F (fig. 6) the journal bearing at the crack side of the rotor was replaced by a ball bearing. The load was afforded by a ball bearing, too. To reduce the necessary amount of the external force the diameter of the shaft at the crack position was reduced to a diameter of 45 mm with a cut radius of 5 mm. For crack initiation a 4 mm deep cut was sawn with a thin wire of 70 µm diameter (fig. 7).

For crack propagation an external force of 5000 N and 3000 N, depending on the crack depth, was necessary during about 3 h. The crack propagation was controlled by observing the twice per revolution resonance amplitude near the crack position using a 2-channel Fast-Fourier-Analyser. The rotating speed was equal to correspon-

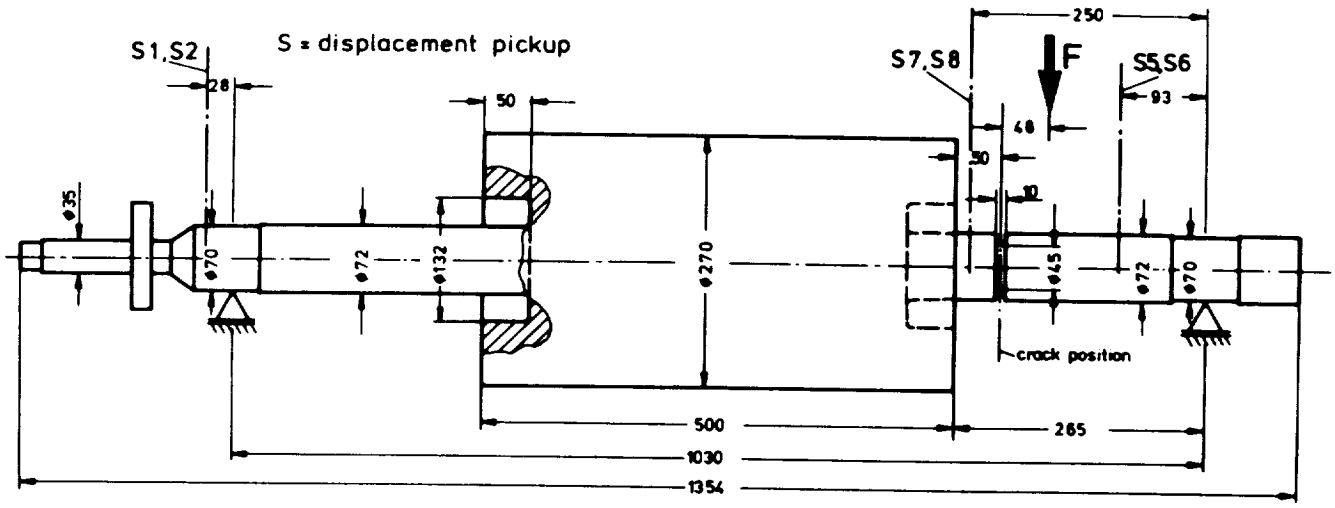

Figure 6. - Experimental rotor.

ding resonance frequency. Unfortunately, two cracks came into existence. Probably on the opposite side of the cut a small groove was the cause for the second crack. Therefore, the comparison of the theoretical and experimental results is uncertain.

For the theoretical calculations we have assumed a linear shape of the crack ground (fig. 7) and a crack depth of 45 % of the diameter. We intend to carry out additional experiments with this rotor, e.g. with different unbalances. Therefore, we did not break the shaft at the crack position.

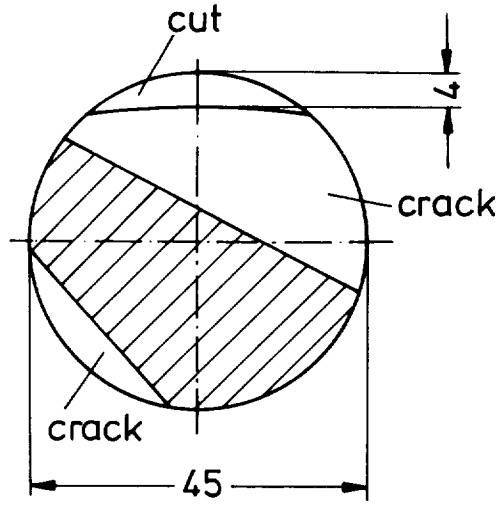

Figure 7. - Cross-section at crack position.

Theoretical Model of the Rotor

The vibrational behavior of the rotor has been caluclated with the FEM and the transfer matrix method. To make use of the crack model with L = T , the geometry in the neighbourhood of the crack had to be modified. We have assumed one element of a diameter of 64 mm and a length of 32 mm (fig. 8). This gives the same flexural shape as the real geometry.

The change of stiffness due to the crack is the same as in the case of the original rotor. But difficulties result from the uncertain knowledge of the stiffness and damping coefficients of the journal bearings.

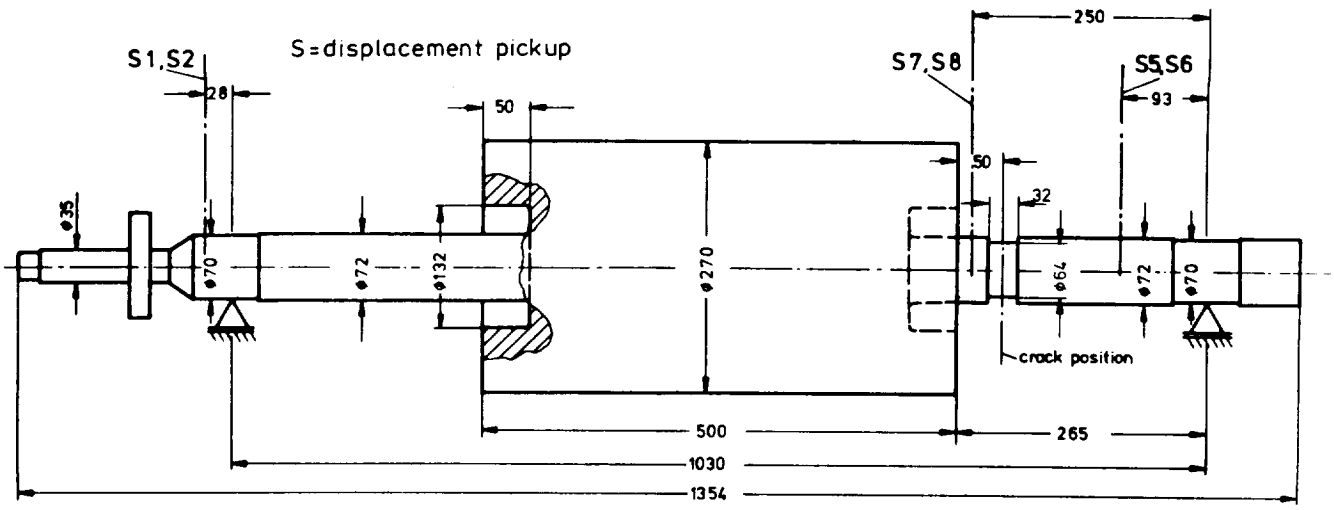

Figure 8. - Rotor model for calculation.

The vibrations excited by a crack depend severely on the curvature of the eigenmodes at the crack position and on the weight influence (see ref. 13). If

$$\int_0^{\ell} g\,\mu(x)\,Y_{ok}(x)\,dx \approx 0 \quad , \tag{5}$$

g - gravity constant,

$\mu(x)$ - shaft weight/unit length,

Y_{ok} - eigenmode,

the crack does not excite any vibration. This is approximately the case for the second eigenmodes in the horizontal and the vertical plane (figs. 9 to 12) and accordingly for the third and fourth complex eigenmode of the complete system (fig. 13), too.

So, already the eigenmodes give an idea about the speed ranges in which crack-excited vibrations can be expected.

THEORETICAL AND EXPERIMENTAL RESULTS

Eigenfrequencies and Eigenmodes

The results of the numerical investigation of the vibrational behavior of the cracked rotor are obtained by using the uncoupled eigenmodes of the conservative system (figs. 10 and 12). The modal transformation includes the complete bearing stiffness and damping coefficients.

Figures 8 and 9 and figures 10 and 11 show, that the difference between the calculated eigenfrequencies of the uncracked and the cracked rotor amounts to approximately 3 %. The measured frequencies in figure 14 (uncracked) and figure 16

(cracked) differ approximately 12 %. This indicates that the assumed mean stiffness reduction in the calculation of the eigenfrequencies is too small. In the case of the uncracked rotor the measured and calculated eigenfrequencies are in good agreement. For comparison only the first few eigenmodes of the complete coupled nonconservative rotor (fig. 13) are calculated with FEM.

Rotor with Cut

An interesting experimental result is depicted in the figures 14 and 15. The cut with a depth of approximately 10 % of the diameter has no influence on the once per revolution vibration amplitudes. This corresponds to the theory for a gaping crack. (The small difference may be the result of a change in the distortion due to the storage during some days.) The amplitudes at low speeds seem to be due to the runout. The rotor is neither balanced nor equipped with an additional unbalance. The twice per revolution vibration amplitudes may also contain runout, but less than 1 µm. The resonance amplitude increases up to 16 µm. One or two additional resonance frequencies can be observed at higher speeds. The small amplitudes of these resonance vibrations can be explained by the weight influence (see eq. (5)). The rotor with cut has not been theoretically investigated.

Cracked Rotor

As mentioned, the missing knowledge of the exact bearing stiffness and damping coefficients is a problem when calculating the vibrational behavior of rotating shafts. The theoretical model of this rotor does not include the measured rigid-body eigenmode at 2400 rev/min (figs. 16 and 18). The resonance frequency at 4000 rev/min is not theoretically determinable, too. But for crack detection this effects are of secondary order. The comparison of the measured (figs. 17 and 19) and calculated (figs. 16 and 18) once per revolution vibration amplitudes shows a very good agreement at both mesuring planes S 56 and S 78. We indeed expected a good agreement, but this exact agreement must be an accidental one.

On the other hand, between the measured and calculated twice per revolution resonance amplitudes exist a factor of 2. This is to be explaned with the two cracks in the shaft. The stiffness changes two times per revolution and therefore we have a greater excitation of twice per revolution vibrations than the crack model delivers.

In figures 20 and 21 the complete frequency spectrum of the rotor with cut is compared with the spectrum of the cracked rotor. The scales are the same. This representation gives a good survey of the change of the vibrational behavior due to the crack.

At the rotational speed of 7000 rev/min a resonance vibration appeared with a frequency of approximately 3500 rev/min for a very short time. Until now we have no explanation for this effect.

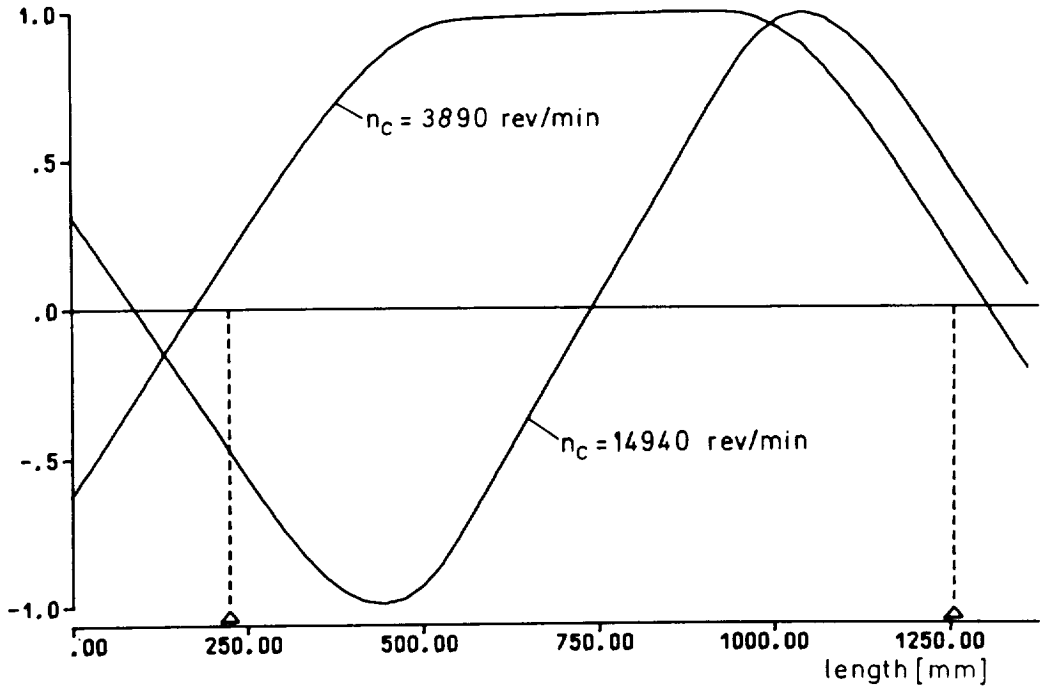

Figure 9. - Horizontal eigenmodes of undamped system (uncracked rotor).

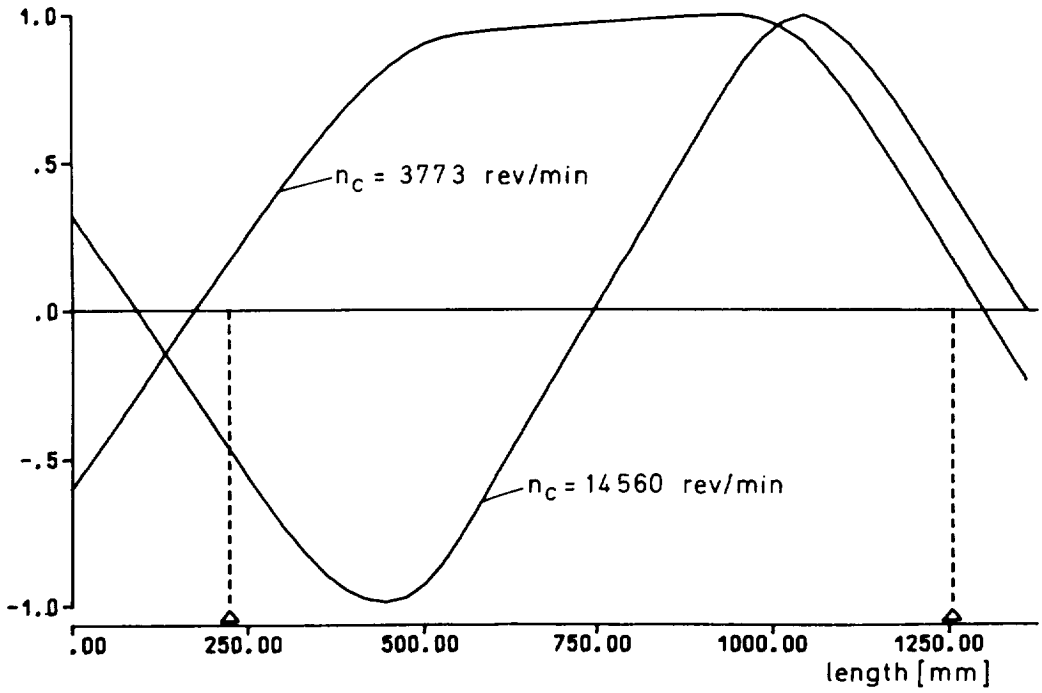

Figure 10. - Horizontal eigenmodes of undamped system (cracked rotor).

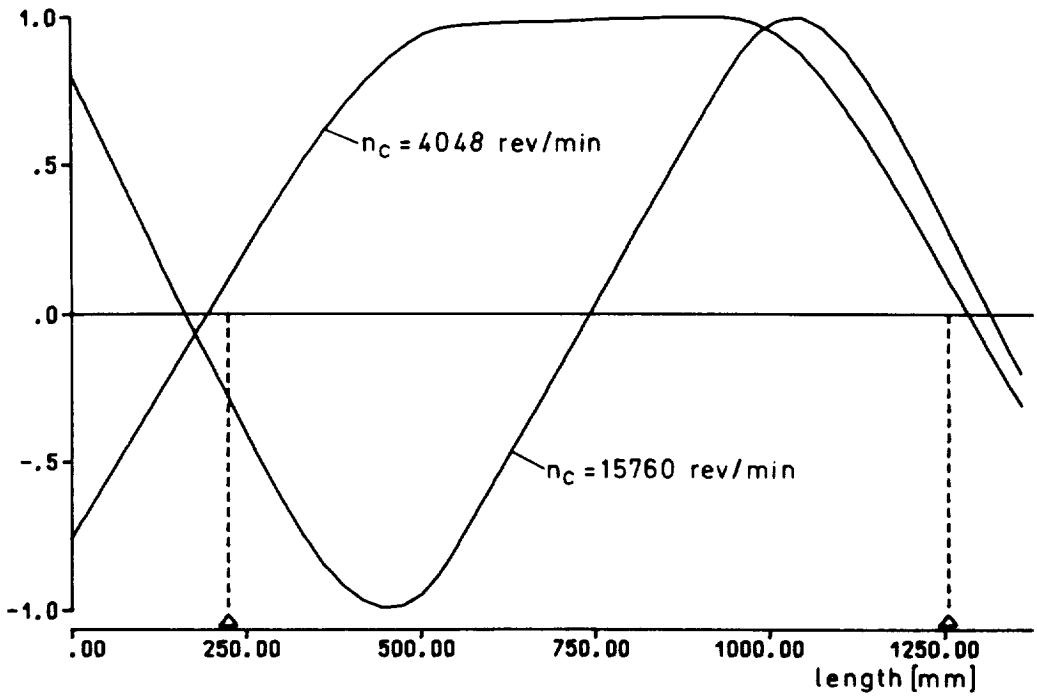

Figure 11. - Vertical eigenmodes of undamped system (uncracked rotor).

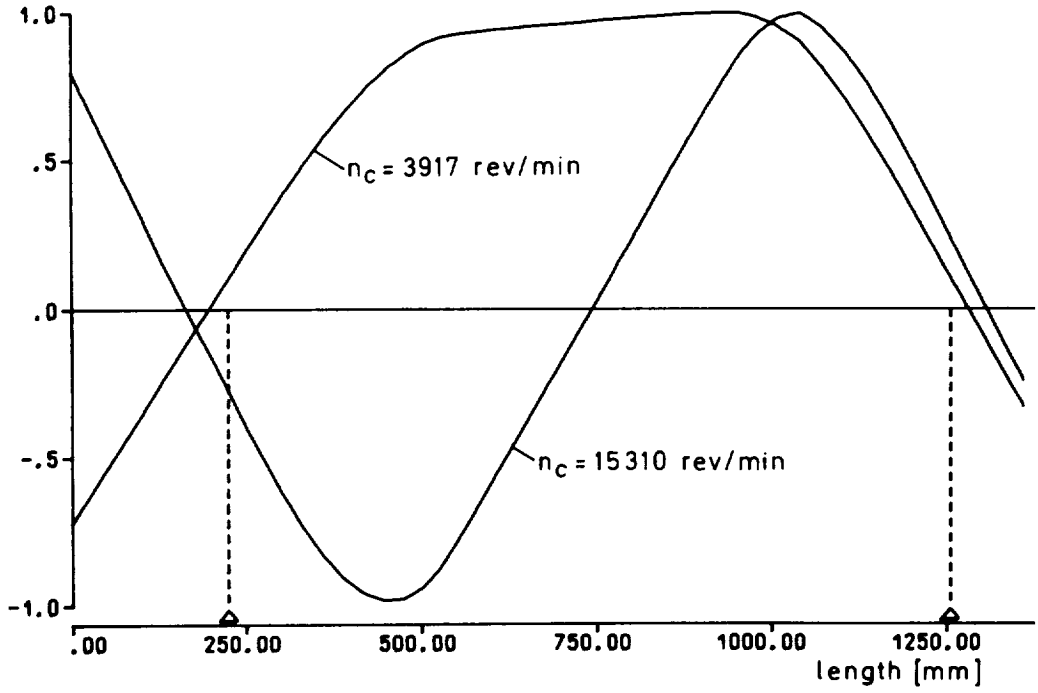

Figure 12. - Vertical eigenmodes of undamped system (cracked rotor).

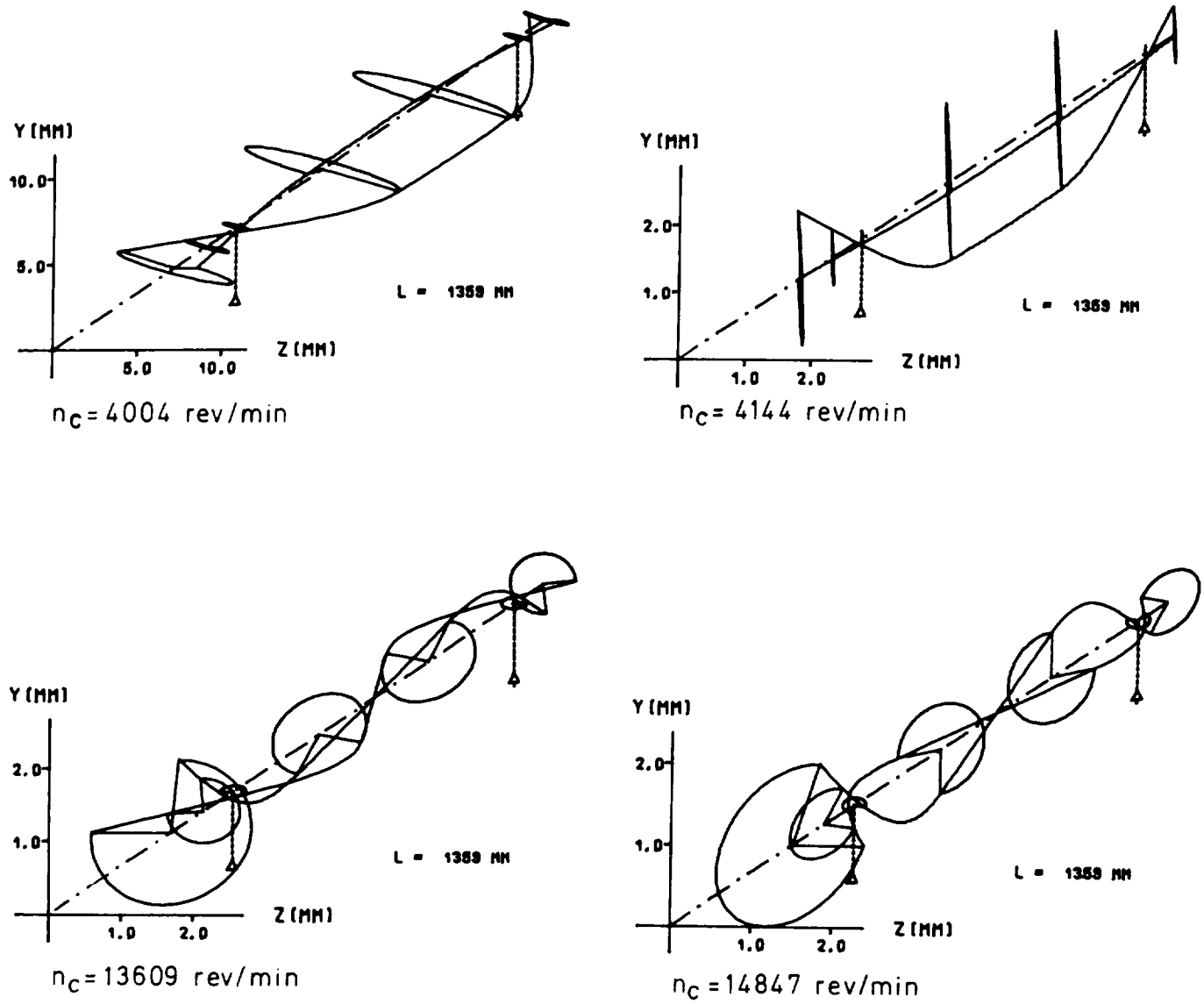

Figure 13. - First four complex eigenmodes of complete damped system (uncracked rotor).

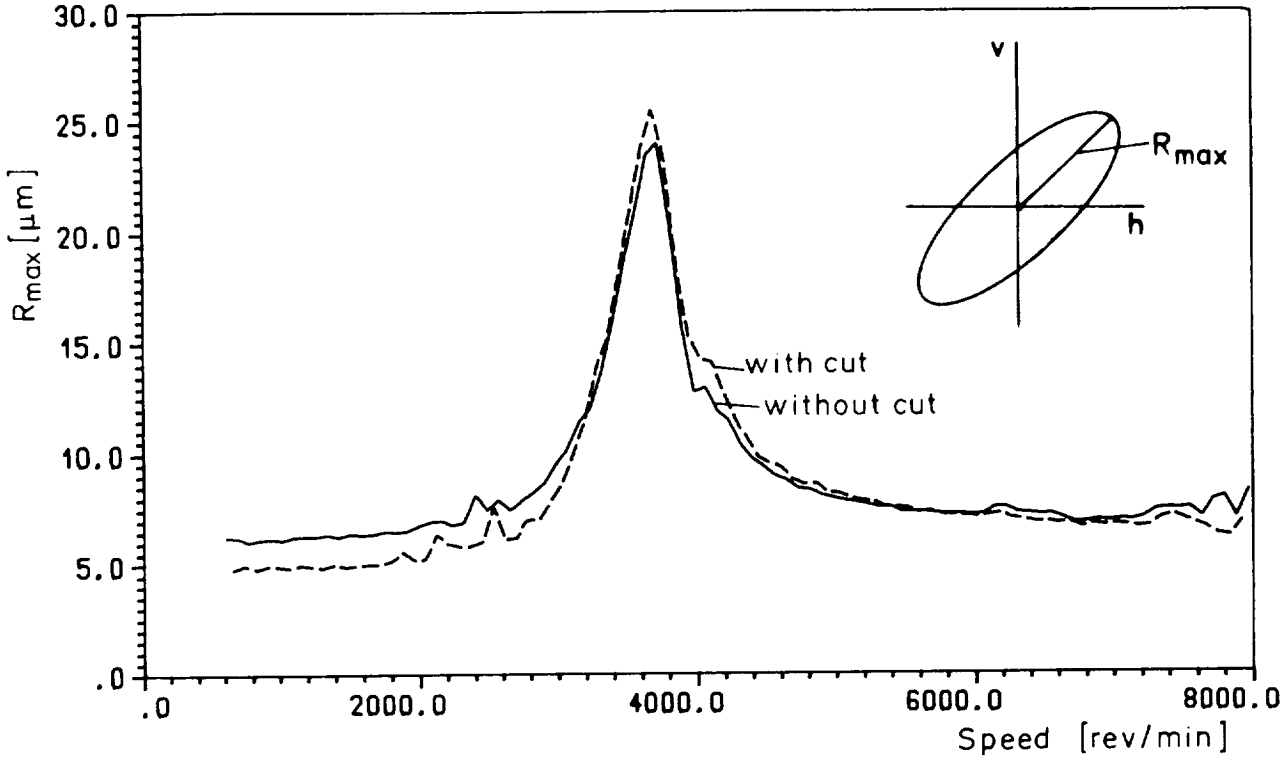

Figure 14. - Once-per-revolution vibration amplitudes of rotor without and with cut measured at position S78.

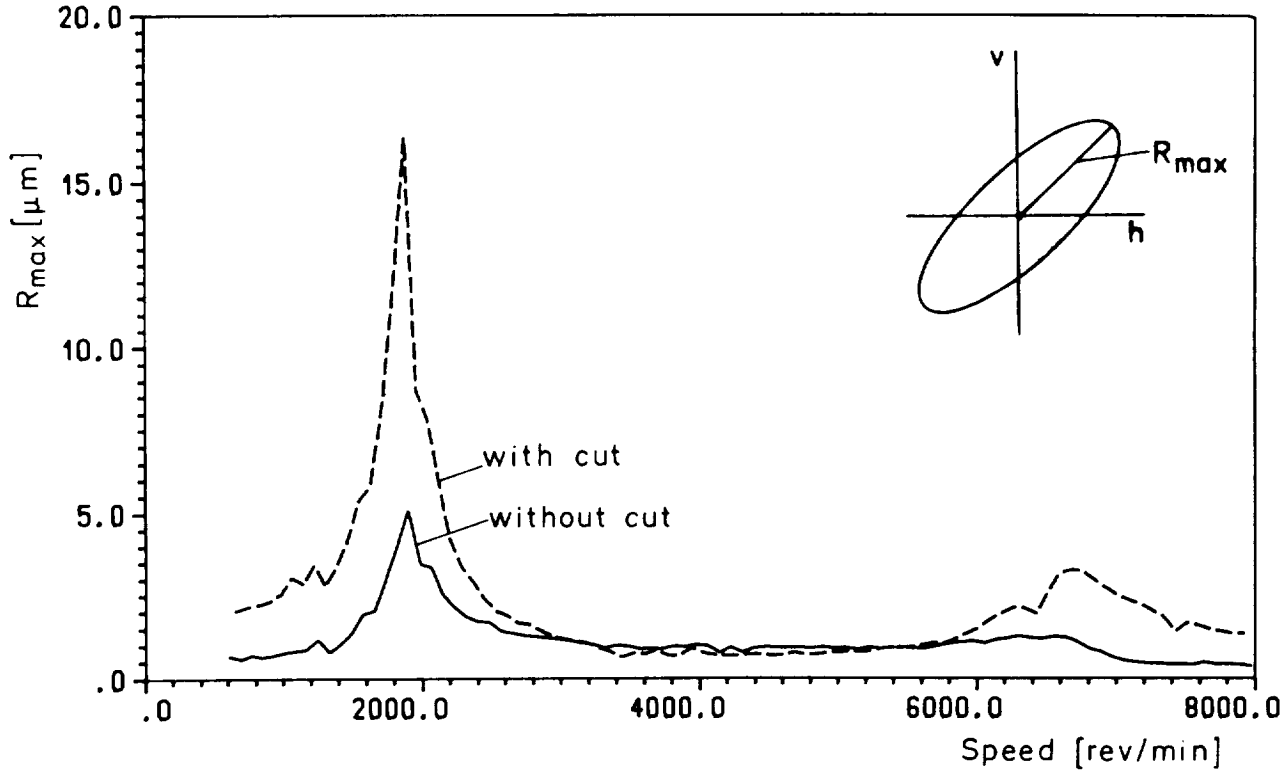

Figure 15. - Twice-per-revolution vibration amplitudes of rotor without and with cut measured at position S78.

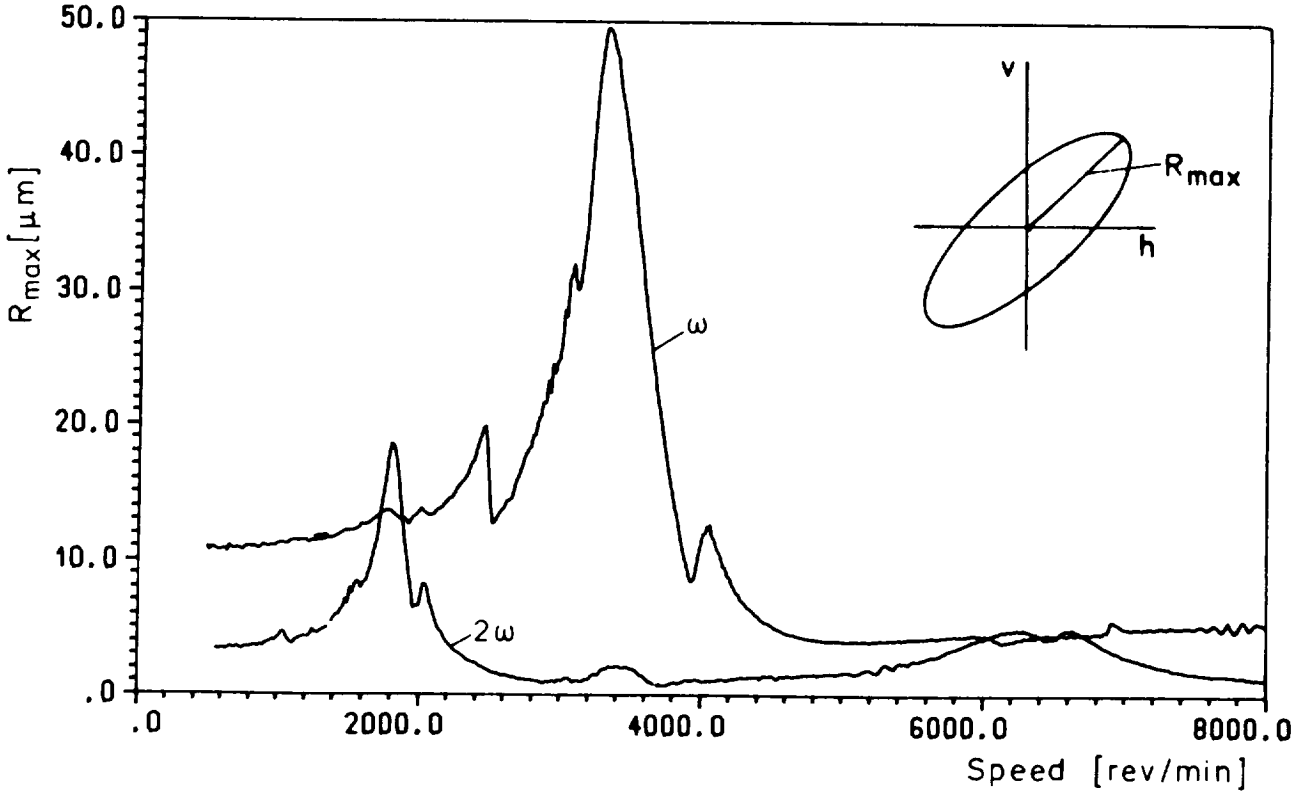

Figure 16. - Measured vibration amplitudes of cracked rotor at position S56.

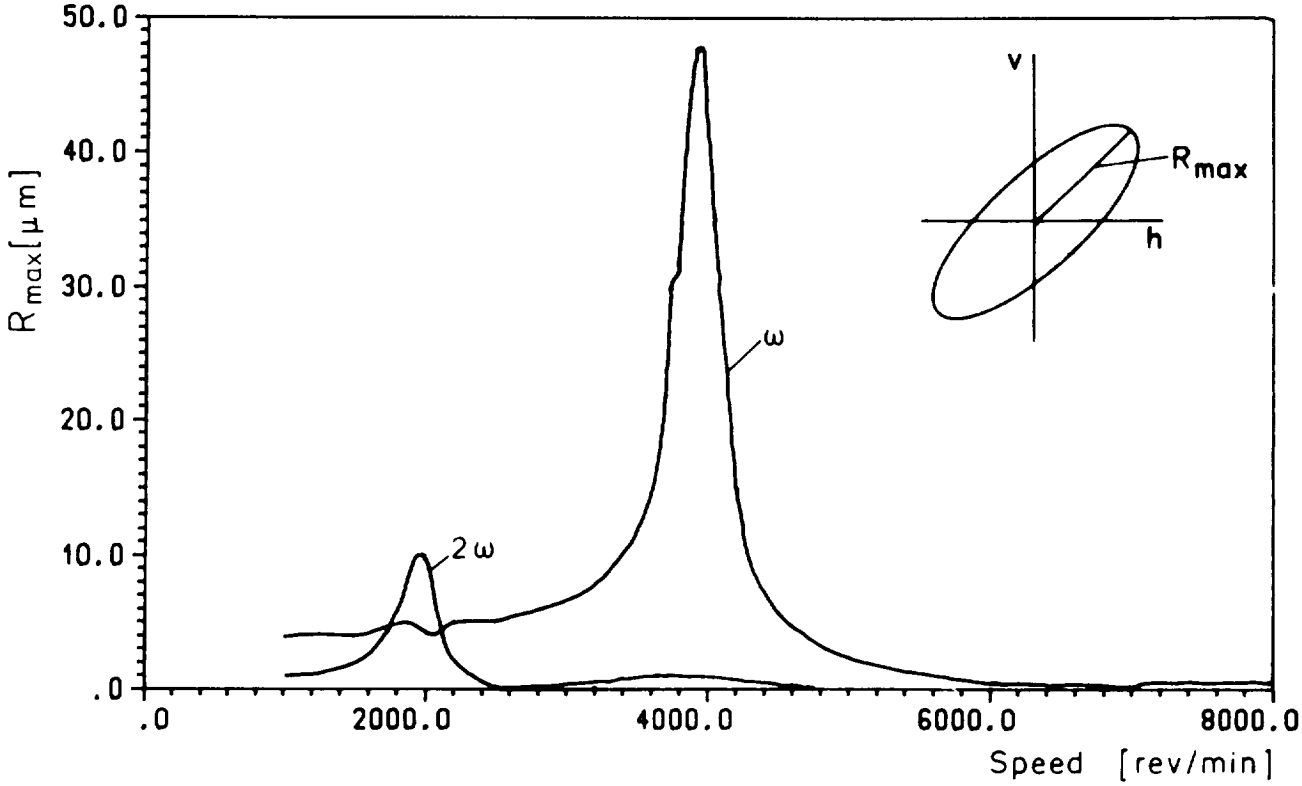

Figure 17. - Calculated vibration amplitudes of cracked rotor at position S56 (crack depth 45 % of diameter).

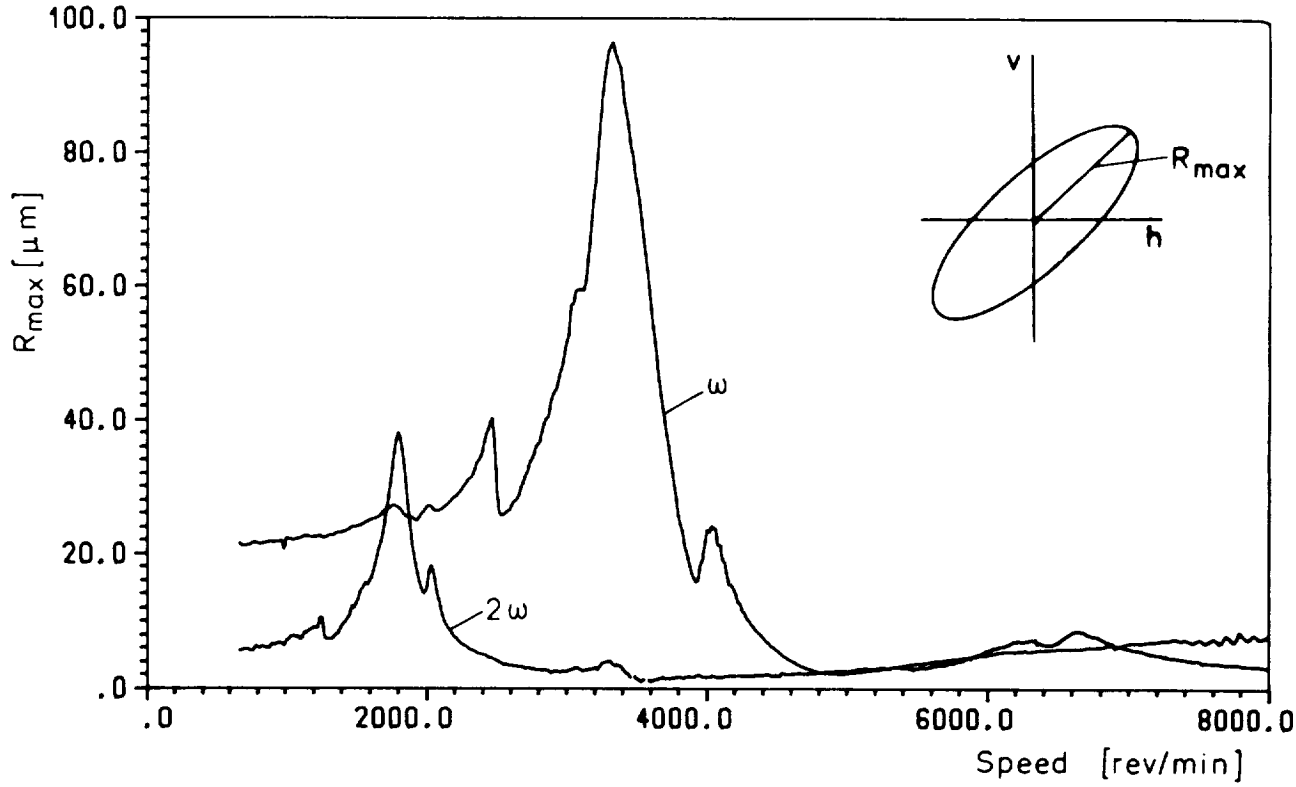

Figure 18. - Measured vibration amplitudes of cracked rotor at position S78.

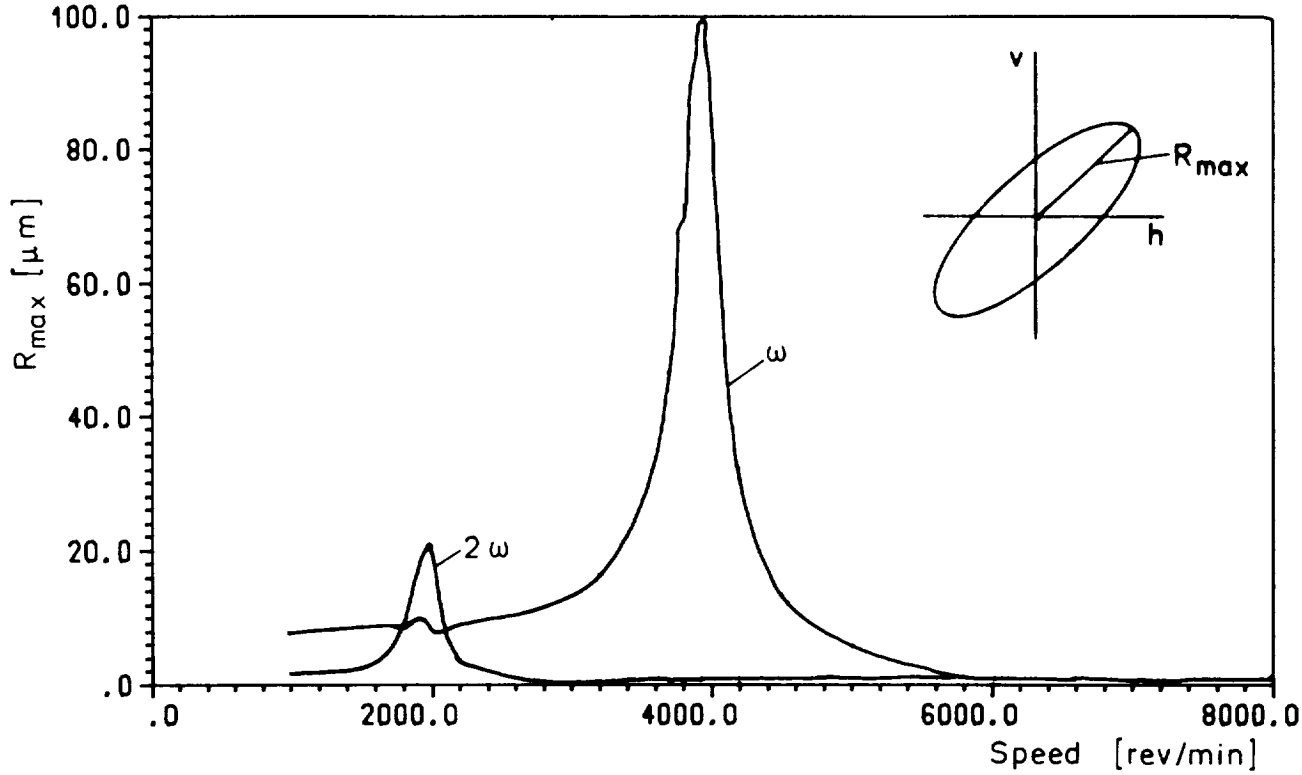

Figure 19. - Calculated vibration amplitudes of cracked rotor at position S78 (crack depth 45 % of diameter).

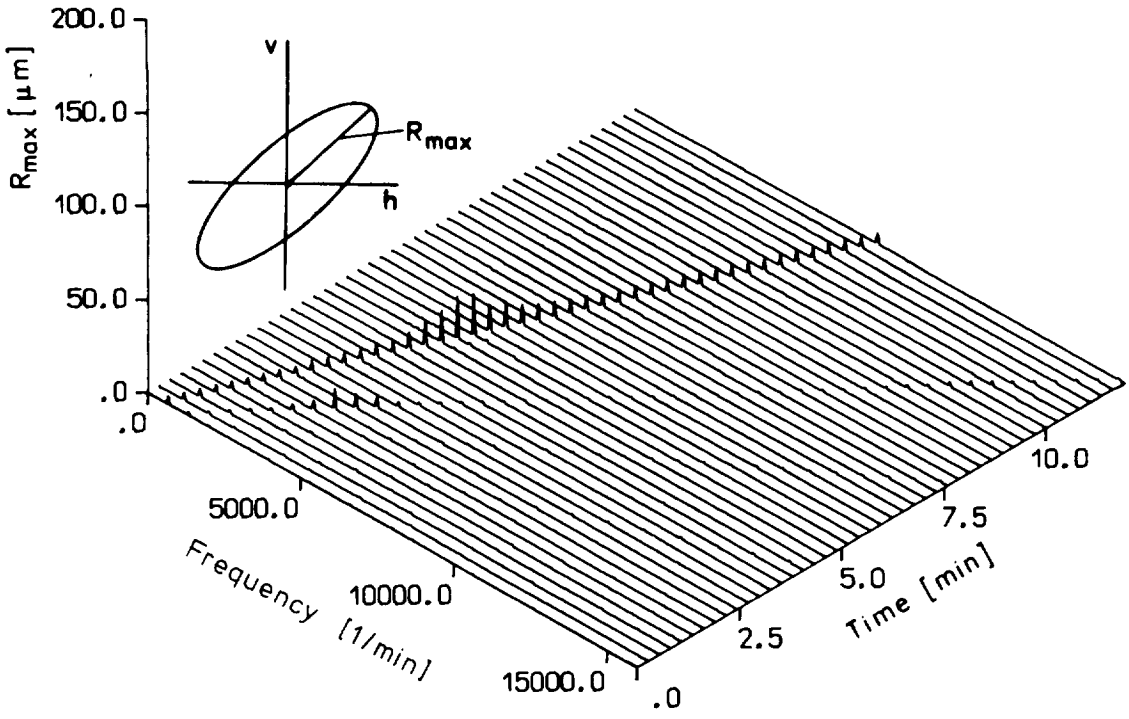

Figure 20. - Frequency spectrum of rotor with cut.

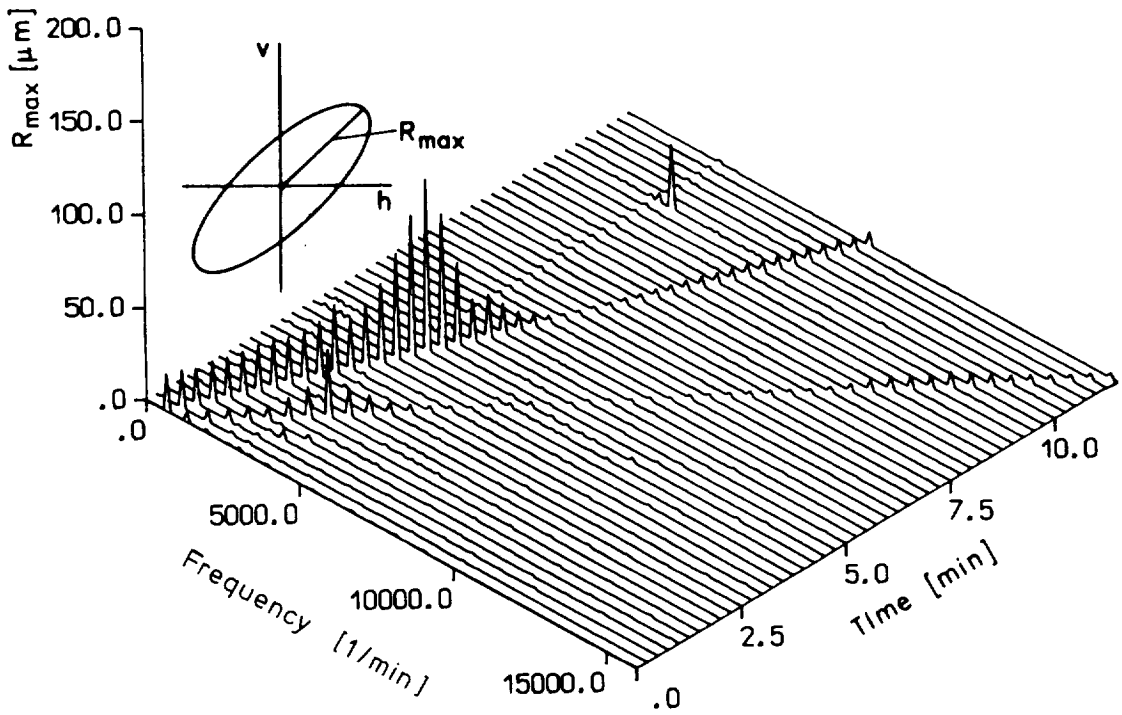

Figure 21. - Frequency spectrum of cracked rotor.

CONCLUSION

The comparison of calculation and measurement shows in principle that it is possible to predetermine the vibration amplitudes excited by a crack. But at the same time this investigation shows the problems in modelling the system. The developed crack model seems to be useful.

For crack supervision the phase should be taken into account, too, because the amplitude of the sum of the original vibration and the vibration due to crack can become smaller with crack propagation.

In the future the influence of unbalance is to be investigated. Our calculations have shown, that this influence frequently is small for greater turbine rotors because the statical deflection is greater than the vibration amplitudes. But in rotors constructed like this experimental rotor an influence can be expected. Here the vibration amplitudes at crack position have the same magnitude like the statical deflection.

REFERENCES

1. Haas, H.: Großschäden durch Turbinen- oder Generatorläufer, entstanden im Bereich bis zur Schleuderdrehzahl. Der Maschinenschaden, 50. Jahrgang, Heft 6, 1977, pp. 195-204.

2. Stodola, A.: Dampf- und Gasturbinen. Springer, Berlin, 5. Auflage, 1922, pp. 931.

3. Kellenberger, W.: Biegeschwingungen einer unrunden, rotierenden Welle in horizontaler Lage. Ingernieur-Archiv, XXVI, 1958, pp. 302-318.

4. Tondl, A.: The Effect of Unequal Moments of Intertia of the Shaft Section on the Motion and Stability of a Rotor. Some Problems of Rotor Dynamics, 1st ed., Chapman & Hall, London.

5. Bishop, R.E.D. and Parkinson, A.G.: Second Order Vibration of Flexible Shafts. Phil. Trans. of Royal Society of London, vol. 259, no. 1095, 1965.

6. Mayes, I.W. and Davies, W.G.R.: A Method of Calculating the Vibrational Behaviour of Coupled Rotating Shafts Containing a Transverse Crack. Second Int. Conference Vibrations in Rotating Machinery, University of Cambridge, 2-4 Sept., 1980.

7. Inagaki, T.; Kanki, H.; and Shiraki, K.: Transverse Vibrations of a General Cracked-Rotor Bearing System. ASME Paper No. 81-Det-45, Sept. 1981.

8. Henry, T.A. and Okah-Avae, B.E.: Vibrations in Cracked Shafts. Conf. on Vibrations in Rotating Machinery, University of Cambridge, Sept. 1976, pp. 15-19.

9. Buerhop, H.: Zur Berechnung der Biegesteifigkeit abgesetzter Stäbe und Wellen unter Anwendung von finiten Elementen. VDI-Fortschrittsberichts, Reihe 1, Nr. 36, 1975.

10. Ziebarth, H.; Schwertfeder, H. und Mühle, E.-E.: Auswirkung von Querrissen auf das Schwingungsverhalten von Rotoren. VDI-Berichte 320, 1978, pp. 37-43.

11. Fehlberg, E.: Neue genaue Runge-Kutta-Formeln für Differentialgleichungen zweiter Ordnung bzw. n-ter Ordnung. ZAMM 40, 1960, pp. 449-455.

12. Grabowski, B.: Zur modalen Simulation des instationären Schwingungsverhaltens von Turboläufern. VDI-Fortschrittberichte, Reihe 11, Nr. 25, 1976.

13. Grabowski, B.: The Vibrational Behavior of a Turbine Rotor Containing a Transverse Crack. Trans. ASME, J. Mech. Design., vol. 102, Jan. 1980, pp. 140-146.

14. Grabowski, B.: Das Schwingungsverhalten eines angerissenen Turbinenläufers. VDI-Bericht Nr. 320, 1978, pp. 31-36.